View metadata, citation and similar papers at core.ac.uk
brought to you by CORE
provided by Apollo

Growth of continuous Graphene by open Roll-to-Roll Chemical Vapor Deposition

Guofang Zhong,[1,*] Xingyi Wu,[1] Lorenzo D'Arsie, [1] Kenneth B. K. Teo,[2] Nalin L. Rupesinghe,[2] Alex Jouvray,[2] John Robertson[1]

[1]*Department of Engineering, University of Cambridge, Cambridge, CB3 0FA, United Kingdom*
[2]*AIXTRON Ltd, Anderson Road, Swavesey, Cambridge CB24 4FQ, United Kingdom*
* gz222@cam.ac.uk

We demonstrate the growth of high-quality, continuous monolayer graphene on Cu foils using an open roll-to-roll (R2R) chemical vapor deposition (CVD) reactor with both static and moving foil growth conditions. N_2 not Ar was used as carrier gas to reduce process cost, and the concentrations of H_2 and CH_4 reactants were kept below the lower explosive limit to ensure process safety for reactor ends open to ambient. The carrier mobility of graphene deposited at a Cu foil winding speed of 5 mm/min was 5270-6040 $cm^2V^{-1}s^{-1}$ at room temperature (on 50 μm × 50 μm Hall devices). These results will enable the in-line integration of graphene CVD for industrial R2R production.

Chemical vapor deposition (CVD) offers process controllability, scalability and flexibility and is today regarded as the most promising method for industrial production of high-quality, monolayer and continuous graphene for electronic device applications [1-4]. Recently, several roll-to-roll (R2R) CVD systems have been developed for production of graphene on Cu foils [5-9]. R2R growth of multi-layer graphene was first achieved by Hesjedal [5] at 1000°C using atmospheric-pressure (AP-) CVD (feeding gases: Ar, H_2 and CH_4) and then by Yamada et al. [6] at a much lower temperature of 400°C using a low pressure (LP) 20 kW microwave plasma enhanced (PE) CVD (30 Pa, Ar, H_2 and CH_4) system. However, this PECVD method resulted in much lower quality graphene. Kobayashi et al [7] developed a R2R LP-CVD system to grow monolayer graphene by Joule heating of the Cu foils, but the as-grown graphene was non-uniform and discontinuous, with a carrier mobility of ~900 $cm^2V^{-1}s^{-1}$. Ryu et al [8] showed a vertical reactor capable of R2R operation. Finally, Polsen et al [9] reported high-speed R2R graphene production using a concentric tube CVD reactor (1010°C, 4 Torr, He, H_2, C_2H_4). They wrapped a Cu foil helically onto the surface of an inner tube. However, this results in a higher winding speed and more curvature than a straight moving foil, which will inevitably sacrifice the quality and continuity of the as-grown graphene that is detrimental to applications. Bae et al. [10] achieved 30-inch graphene films, but they used a closed CVD reactor.

Therefore, the present R2R CVD systems do not simultaneously fulfill the demands for high quality, monolayer and continuity of the as-grown graphene, which are essential for electronic grade graphene applications [4]. In fact, the existing R2R CVD systems are simply R2R reactors enclosed in leak-proof reactors. They could be classified as batch systems, which produce graphene on Cu foils, coil by coil, but they cannot be integrated into in-line serial production lines with sequential processes before growth (such as Cu foil cleaning, polishing or annealing) and after growth (such as graphene transfer and device manufacture). Thus, the in-line integration of graphene growth for manufacturing requires an open type (OP-) R2R CVD system.

This paper describes the operation of a prototype open R2R CVD reactor (OP-R2R CVD) which uses H_2 and CH_4 as reactants and nitrogen as the carrier gas, operating at atmospheric pressure.

The operation of an atmospheric pressure, OP-R2R CVD graphene reactor has not yet been reported due to the following challenges:

Firstly, ‘open’ means that the CVD system is not air-tight and the processing gases are discharged directly into the ambient. This raises process safety issues due to the use of flammable gases such as H_2 and hydrocarbons like CH_4. The lower explosion limits (LEL) of H_2 and CH_4 in air are 4% and 5%, respectively [11]. This means that all LP-CVD and most AP-CVD conditions cannot be applied to OP- R2R CVD due to the low operation pressure or the high concentrations of H_2 and CH_4 above the LEL [1,10,12-15].

Secondly, if the flammable gas is diluted well below its LEL, atmospheric O_2 may enter the reactor by leakage or diffusion at the openings. The nucleation density of graphene by LP-CVD decreases monotonically with the O_2 partial pressure [16], while the growth rate reaches a maximum at a certain pressure [17]. A high flow rate of a carrier gas such as Ar can be used for open systems to prevent O_2 ingress. However, the comparatively high cost of Ar results in a high cost of ownership for high flow rates. Hence, an alternative to Ar is needed to reduce process costs.

A third point concerns the choice of catalyst. Cu is the standard graphene CVD catalyst, but it must be used near its melting temperature, where its softness means that foil tensioning must be carefully controlled. Ni or Co are other possible catalysts, but are high-cost for a large scale process. Fe is the other low-cost metal. It is stronger, but as a carbide former, it is more difficult to control to give monolayer graphene. Thus, we remain with copper.

Here, we demonstrate the growth of high quality, monolayer and continuous graphene on Cu foils using an OP-R2R CVD reactor (Figure 1). We use N_2 as the carrier gas, and diluted H_2 and CH_4 as the reactant gases. Ar is generally used as the carrier gas because it is inter. Nitrogen is not used in this way because it might be reactive. For example, nitrogen can alter the microstructure of carbon nanotubes, inducing the bamboo morphology [18], and nitrogen can dope graphene in a plasma reactor, but it also introduces defects [19].

We recently produced high quality monolayer graphene with millimeter sized domains by Ar-diluting the main flammable gas of H_2 below its LEL using a traditional closed CVD furnace [20]. Based on this work, Fig. 1 shows the prototype OP-R2R CVD reactor for graphene growth on Cu foils using a mixture of CH_4, H_2 and N_2 (vendor: BOC, purity: 99.999%). In order to dramatically reduce the process cost, N_2 is used as the carrier gas, which is vaporized from liquid N_2 centrally supplied to the lab, instead of the inert gas Ar. The reactor is a vertical quartz tube (25 mm diameter x 300 mm long) furnace with both ends open to air to allow foil transport in and out of the reactor. The vertical design keeps the Cu foil in the center of the quartz tube with a constant foil tension using its own weight, and this allows for thermal expansion or contraction during the CVD process. The inlet gases are supplied from the bottom end of the reactor, Fig. 1(a). During the CVD process, by virtue of the gas flow and over-pressure, the gases are released into the ambient through both ends of the reactor, and it is this flow of gas which prevents the oxygen ingress to the reactor from the ambient.

The as-received commercial Cu foils, in the form of a strip (purity: 99.9%, Size: 20 m × 12 mm × 40 μm, vendor: Goodfellow, part no.: CU000424) are directly used as catalytic substrates

for graphene growth. The whole CVD process for graphene growth includes three stages (Fig. 1(c). First, a Cu foil is manually wrapped onto the bottom roller, loaded through the reactor and onto the top roller. The furnace is then heated up to 1010-1070°C at 50°C/min with a N_2 flow rate of 5-10 slm for 25 min. In this stage, the Cu foil inside the furnace is annealed. Second, the graphene growth is initialized by adding 0.5-5 sccm CH_4 and 80-160 sccm H_2 to the N_2 flow. To avoid forming a flammable mixture, the total flow rate of the flammable gases are controlled to below 2.5% when combined with the N_2 carrier gas. For static growth with a stationary Cu foil, the growth time is typically 40 min. For dynamic growth, with the Cu foil wound to the top roller at a certain speed, 70-90 min was used such that a reasonable length (eg. 2x reactor length) of Cu foil could be transported through the growth zone. To end the process, the growth is terminated and the sample is cooled down by switching off the CH_4 flow and the heater power. After the temperature drops below 100°C, the H_2 and N_2 flows are stopped and the as-grown foil strip is removed. The strip is then labelled every centimetre relative to the bottom of the furnace for analysis, as shown in Fig. 1a.

Scanning electron microscopy (SEM, Philips XL30 SFEG and Carl Zeiss Sigma), micro-Raman spectroscopy (Renishaw inVia) and optical microscopy (OM, Nikon ECLIPSE LV150N) are used to characterize the as-grown and the transferred graphene samples. The carrier mobility of the transferred graphene is measured by Hall effect of a Van der Pauw structure [21]. The details of graphene transfer were reported previously [20].

Before the dynamic OP-R2R growth test, we first needed to develop and optimize a static condition for the growth of high quality, monolayer, continuous graphene within a reasonable time. As mentioned earlier, the challenge is the ingress of O_2 from the air at both open ends. Thus, the size of the openings and the flow rate of the carrier gas were optimised to enable the growth of graphene.

Fig. 2(a) shows a series of SEM images of a graphene sample prepared under an optimized condition: 1010°C, 2 sccm CH_4, 160 sccm H_2, 8 slm N_2 in 20 min. Continuous graphene can be grown on Cu foils between the 10th and 25th cm (Fig. 2a(ii-ix)), while non-continuous graphene domains can be observed at both ends of the continuous graphene (Fig. 2(i,x)). Increasing the growth time does not further increase the length of the continuous graphene zone; however, reducing the growth time shortens the continuous graphene zone [22,23]. This agrees with the kinetic study of graphene growth: continuous graphene can only grow under a high temperature and the higher the temperature, the shorter the growth time [22,24]. We note that reducing the CH_4 flow rate below 0.5 sccm, the as-grown graphene is not always continuous despite the extension of growth time to 60 min, while increasing the CH_4 flow above 5 sccm leads to the growth of multilayer graphene [13,25]. Fig. 1(d) also shows that the actual temperature profile is asymmetrical and the highest temperature position is shifted upwards from the furnace center. This is because (1) a high flow rate of “cold” N_2 is introduced into the relatively small quartz tube from the bottom compared to in our conventional *closed*-type CVD (carrier gas: 4 slm Ar, quartz tube: 50mm in diameter) - this cools the lower half [20]; (2) the vertical configuration of the furnace results in rising hot gases compared to a horizontal furnace. Fig 2(b) shows SEM images of the resulting samples.

Fig. 3a(i-ii) shows two OM images of graphene transferred onto SiO_2 from different positions on the Cu foil. It can be seen that the graphene is continuous and uniform in color, which indicates uniformity in thickness. Fig. 3a(iii) shows Raman spectra of graphene samples transferred from different positions of the Cu foil; we deduce that this is high quality, monolayer,

continuous graphene (11st -25th cm) from the following: (1) there is no obvious D band at ~1350 cm^{-1} which is related to the defects in graphene, and (2) the appearance of the sharp and intense 2D peak at ~2690 cm^{-1}, which is at least 2.6 times as high as the G peak at ~1590 cm^{-1} (see Fig. 3a(iv)) [26]. The absence of a D peak also indicates that the nitrogen carrier gas does not introduce defects. Fig. 3(a) also shows that at the macro scale, homogeneity of graphene in layer number and quality was obtained along the strip of Cu foil.

The static growth experiment shows that graphene can be grown in the zone located between the 10th - 25th cm from the bottom of the reactor. Therefore, to ensure the foil experiences a growth time of at least 20 minutes through this 150 mm growth zone, a maximum winding speed of 7.5 $mm \cdot min^{-1}$ is derived. For this demonstration, we initially use a speed of 10 mm every 1.5 minutes (6.67 $mm \cdot min^{-1}$) which may grow graphene, but not as a continuous film. To allow a longer time in the growth zone, the winding speed is decreased to 5 $mm \cdot min^{-1}$, then we obtain continuous graphene on the Cu foil strip, using a reactor temperature of 1070C.

Fig. 2(b) shows a series of SEM images of a graphene sample dynamically grown on a Cu foil at a winding speed of 5 $mm \cdot min^{-1}$ for a total growth time of 84 min. For the dynamic growth, the same gas flows of 2 sccm CH_4, 160 sccm H_2, 8 slm N_2 ratios are used as for the static case. The maximum temperature is slightly higher at 1070°C. The Cu foil wound outside the furnace (36th - 55th cm) is fully covered with continuous graphene; however, there are some white spots on the sample compared to the statically grown graphene. The white spots have been identified by others as oxides from impurity elements, which can act as nucleation or etching centers of graphene [2,27] At positions below the 20th cm, we can tell the graphene is dis-continuous; however, unlike Fig. 2(a), we can hardly observe any individual graphene domains. Instead, discontinuous graphene bands can be observed, as shown in Fig. 2(b). We attribute this to the fact that in dynamic growth, the Cu foil is not being annealed for a length of time prior to growth; here, the Cu foil is continuously exposed to the growth mixture and being heated up and down as it passes through the reactor. This applies to the foil section from 0 to 42nd cm which lies outside the reactor during the initial heating up period, and is only transported through the reactor with the growth gases are flowing. We surmise that without the annealing step, the Cu foil is not completely reduced, its surface is not reconstructed nor smoothened, and surface contaminations remain as graphene is grown immediately. Therefore, the Cu foil surface morphology, such as the surface defects and the rolling marks will inevitably affect the nucleation and growth of graphene.

Unlike a conventional closed-type CVD reactor, we can immediately tell if the graphene film was continuous or not simply by visually inspecting the foil when it exits the R2R CVD reactor. As shown in Fig. 2(c), when we start to wind the annealed Cu foil (the part inside the reactor during the initial heating stage) out of the reactor, this section of foil always gets oxidized as it exits the reactor which tarnishes the shiny Cu surface and leaves visible brown bands on the foil. This occurs because as the process gases are discharged into the air at the reactor exit, where the temperature is still high enough (~124ºC measured by a type K thermocouple) to mildly oxidize the Cu. As the foil moves, 10-12 min later (corresponding to ~60 mm length), the oxidation of Cu becomes weaker and weaker. This indicates that graphene is forming and therefore preventing that Cu surface from oxidising, but is discontinuous in nature. Finally, the Cu foil no longer becomes oxidized, implying that continuous graphene has formed which protects the Cu surface from oxidation [28].

The graphene dynamically grown on Cu foil was also transferred onto SiO_2/Si substrates. Fig. 3(b) shows three OM images of transferred graphene and the corresponding Raman spectra. The images show no visible differences from the statically grown graphene. However, the Raman 2D/G peak intensity ratios are decreased, but still >1 (Fig. 3a(iv)). Combining the Raman data, SEM and OM observations, we can still conclude that high quality, monolayer and continuous graphene has been produced using the dynamic process through the R2R reactor. A larger D Raman band appears at the 35th cm position in Fig. 3b(iv), implying a stronger quality degradation from this point on. This is evidence that the graphene reacts with O_2 from the air during the very long cooling period at the position where it is just located at the exit of the reactor. As mentioned earlier, the advantage of our reactor is that it allows in-line integration, and therefore by including Cu foil pretreatments such as acid pickling, electropolishing, and/or simply adding an annealing zone to the reactor), the graphene quality can be further improved.

A typical SEM image of the grains is shown in Fig 4. The grain size is ~20 µm. The growth time was quite long, so that there is very high coverage fraction and the grains are well closed up. On the other hand, to measure effective grain size and grain density, we halt growth before grains fully close together and observe the grain size and density by the optical or SEM contrast [20,29].

To measure carrier mobilities, several Hall effect devices in the form of Van der Pauw structures are fabricated using the dynamically grown graphene. The measurement method is the same as used previously [20]. We also calibrated our results of commercial samples of known mobility. We found a carrier mobility is as high as 5270-6040 $cm^2V^{-1}s^{-1}$ at room temperature, measured at different points, which is about 6 times as high as the graphene produced by the closed-type R2R CVD [7]. This confirms that using N_2 as carrier gas instead of Ar does not degrade graphene quality. Moreover, it is significantly higher than most of the graphene samples prepared under a low H_2 concentration (<4%) by conventional CVD [8,20,30-31]. As the Hall device in our mobility measurement is as large as 50 µm × 50 µm, the high observed mobility is a strong indication of the high quality and spatial uniformity of the samples.

We believe that the high reactor temperature of up to 1070ºC enabled the growth of high quality graphene on Cu foils without the need to pre-anneal in a non-carbon atmosphere [32-34]. It is also possible that a small residual O_2 concentration in the open reactor assisted in the nucleation and formation of high quality graphene [20], to be confirmed by further investigation.

In summary, high quality, monolayer, continuous graphene films have been produced using an open R2R CVD reactor under static and moving foil conditions. By using N_2 produced from a bulk liquid source as the carrier gas, H_2 and CH_4 as the reactant gases at concentrations below the LEL, the process cost is dramatically reduced and safety assured. The open R2R reactor allows in-line graphene growth integration and will enable large scale production of electronic grade graphene.

The authors acknowledge funding from the EC project GRAFOL, grant 285275 and EPSRC grant Graphted EP/K0166636.

References

1. X. S. Li, W. W. Cai, J. H. An, S. Kim, J. Nah, D. X. Yang, R. Piner, A. Velamakanni, I. Jung, E. Tutuc, S. K. Banerjee, L. Colombo, and R. S. Ruoff, Science **324**, 1312 (2009).
2. I. Vlassiouk, M. Regmi, P. F. Fulvio, S. Dai, P. Datskos, G. Eres, S. Smirnov, ACS Nano **5**, 6069 (2011)
3. K. S. Novoselov, V. I. Falko, L. Colombo, P. R. Gellert, M. G. Schwab, K. Kim, Nature **490** 192 (2012)
4. S. Hofmann, P. Braeuninger-Weimer, and R. S. Weatherup, J. Phys. Chem. Lett. **6**, 2714 (2015).
5. T. Hesjedal, Appl. Phys. Lett. **98**, 133106 (2011).
6. T. Yamada, M. Ishihara, J. Kim, M. Hasegawa, and S. Iijima, Carbon **50**, 2615 (2012).
7. T. Kobayashi, M. Bando, N. Kimura, K. Shimizu, K. Kadono, N. Umezu, K. Miyahara, S. Hayazaki, S. Nagai, Y. Mizuguchi, Y. Murakami, and D. Hobara, Appl. Phys. Lett. **102**, 023112 (2013).
8. J. Ryu, Y. Kim, D. Won, N. Kim, J. S. Park, E. K. Lee, D. Cho, S. P. Cho, S. J. Kim, G. H. Ryu, H. A. S. Shin, Z. Lee, B. H. Hong, and S. Cho, ACS Nano **8**, 950 (2014).
9. E. S. Polsen, D. Q. McNerny, B. Viswanath, S. W. Pattinson, and A. J. Hart, Sci. Rep. **5**, 10257 (2015).
10. S. Bae, H. Kim, Y. Lee, X. F. Xu, J. S. Park, Y. Zheng, J. Balakrishnan, T. Lei, H. R. Kim, Y. I. Song, Y. J. Kim, K. S. Kim, B. Ozyilmaz, J. H. Ahn, B. H. Hong, S. Iijima, Nat. Nanotech **5**, 574 (2010)
11. P. A. Carson and C. J. Mumford, *Hazardous chemicals handbook*, 2nd ed. (Butterworth-Heinemann, Oxford ; Boston, 2002), pp.xii.
12. A. Reina, X. T. Jia, J. Ho, D. Nezich, H. B. Son, V. Bulovic, M. S. Dresselhaus, J. Kong, Nano Lett. **9**, 30 (2009).
13. S. Bhaviripudi, X. T. Jia, M. S. Dresselhaus, and J. Kong, Nano Lett. **10**, 4128 (2010)
14. A. W. Robertson and J. H. Warner, Nano Lett. **11**, 1182 (2011).
15. Z. T. Luo, Y. Lu, D. W. Singer, M. E. Berck, L. A. Somers, B. R. Goldsmith, and A. T. C. Johnson, Chem. Mater. **23**, 1441 (2011).
16. Y F Hao, M S Bharathi, L Wang, Y Y Liu, H Chen, S Nie, X H Wang, H Chou, P Kim, J Hone, L Colombo, R Ruoff, Science **342** 720 (2013)
17. T. O. Terasawa and K. Saiki, Appl. Phys. Express **8**, 035101 (2015).
18. C P Ewels, M Glerup, J Nanosci Nanotech 5 1345 (2005); J W Jang, C E Lee, S C Lyu, T J Lee, C J Lee, App Phys Lett **84** 2877 (2004)
19. Y C Lin, C Y Lin, P W Chiu, App Phys Lett **96** 133110 (2010); Y C Lin, P Y Teng, C H Yeh, M Koshino, P W Chiu, K Suenaga, Nanoletts **15** 7408 (2015)
20. X. Y. Wu, G. F. Zhong, L. D'Arsie, H. Sugime, S. Esconjauregui, A. W. Robertson, and J. Robertson, Sci. Rep. **6**, 21152 (2016).
21. A. Venugopal, J. Chan, X. S. Li, C. W. Magnuson, W. P. Kirk, L. Colombo, R. S. Ruoff, and E. M. Vogel, J. Appl. Phys. **109**, 104511 (2011).
22. H. Kim, C. Mattevi, M. R. Calvo, J. C. Oberg, L. Artiglia, S. Agnoli, C. F. Hirjibehedin, M. Chhowalla, and E. Saiz, ACS Nano **6**, 3614 (2012).
23. H. Kim, E. Saiz, M. Chhowalla, and C. Mattevi, New J. Phys. **15**, 053012 (2013).
24. S. R. Xing, W. Wu, Y. A. Wang, J. M. Bao, and S. S. Pei, Chem. Phys. Lett. **580**, 62 (2013).
25. Z. Q. Tu, Z. C. Liu, Y. F. Li, F. Yang, L. Q. Zhang, Z. Zhao, C. M. Xu, S. F. Wu, H. W. Liu, H. T. Yang, and P. Richard, Carbon **73**, 252 (2014).
26. A. C. Ferrari, J. C. Meyer, V. Scardaci, C. Casiraghi, M. Lazzeri, F. Mauri, S. Piscanec, D. Jiang, K. S. Novoselov, S. Roth, and A. K. Geim, Phys. Rev. Lett. **97**, 187401 (2006).
27. W. Guo, B. Wu, Y. T. Li, L. F. Wang, J. S. Chen, B. Y. Chen, Z. Y. Zhang, L. M. Peng, S. Wang, and Y. Q. Liu, ACS Nano **9**, 5792 (2015).
28. C. C. Jia, J. L. Jiang, L. Gan, and X. F. Guo, Sci. Rep. **2**, 707 (2012).
29. X Wu, G Zhong, J Robertson, Nanoscale 8 16427 (2016)
30. Y. F. Hao, M. S. Bharathi, L. Wang, Y. Y. Liu, H. Chen, S. Nie, X. H. Wang, H. Chou, C. Tan, B. Fallahazad, H. Ramanarayan, C. W. Magnuson, E. Tutuc, B. I. Yakobson, K. F. McCarty, Y. W. Zhang, P. Kim, J. Hone, L. Colombo, and R. S. Ruoff, Science **342**, 720 (2013).
31. Y. S. Kim, J. H. Lee, Y. D. Kim, S. K. Jerng, K. Joo, E. Kim, J. Jung, E. Yoon, Y. D. Park, S. Seo, and S. H. Chun, Nanoscale **5**, 1221 (2013).

32. P. R. Kidambi, C. Ducati, B. Dlubak, D. Gardiner, R. S. Weatherup, M. B. Martin, P. Seneor, H. Coles, and S. Hofmann, J. Phys. Chem. C **116**, 22492 (2012).
33. M. Regmi, M. F. Chisholm, and G. Eres, Carbon **50**, 134 (2012).
34. P. Zhao, A. Kumamoto, S. Kim, X. Chen, B. Hou, S. Chiashi, E. Einarsson, Y. Ikuhara, and S. Maruyama, J. Phys. Chem. C **117**, 10755 (2013).

Figure captions:

Fig. 1. (a) Illustration of a prototype open-type R2R CVD reactor for the growth of graphene on Cu foils, (b) a photo taken under an operating condition, (c) the 3-stage CVD process and (d) the temperature profile of the furnace for both stationary and moving foil.

Fig. 2 A series of SEM images of the as-grown graphene grown on (a) a static Cu foil strip and (b) a moving Cu foil strip using the open reactor; (c) a scanned image of a part of the moving Cu foil strip after graphene growth. Growth conditions for (a): 1010°C, 2 sccm CH_4, 160 sccm H_2, 8 slm N_2 for 20 min and for (b): 1070°C, 2 sccm CH_4, 160 sccm H_2, 8 slm N_2 for 84 min. The labels on each image indicates the sampling position when terminating the growth. All of the images have the same scale bar.

Fig. 3. Optical microscopy images and Raman spectra of graphene transferred onto SiO_2 from different positions of the as-grown grpahene/Cu foil samples by (a) static and (b) dynamic growth. The growth conditions are the same as those given in Figure 2.

Fig. 4. Scanning electron microscopy image of graphene grains from the dynamic growth process.

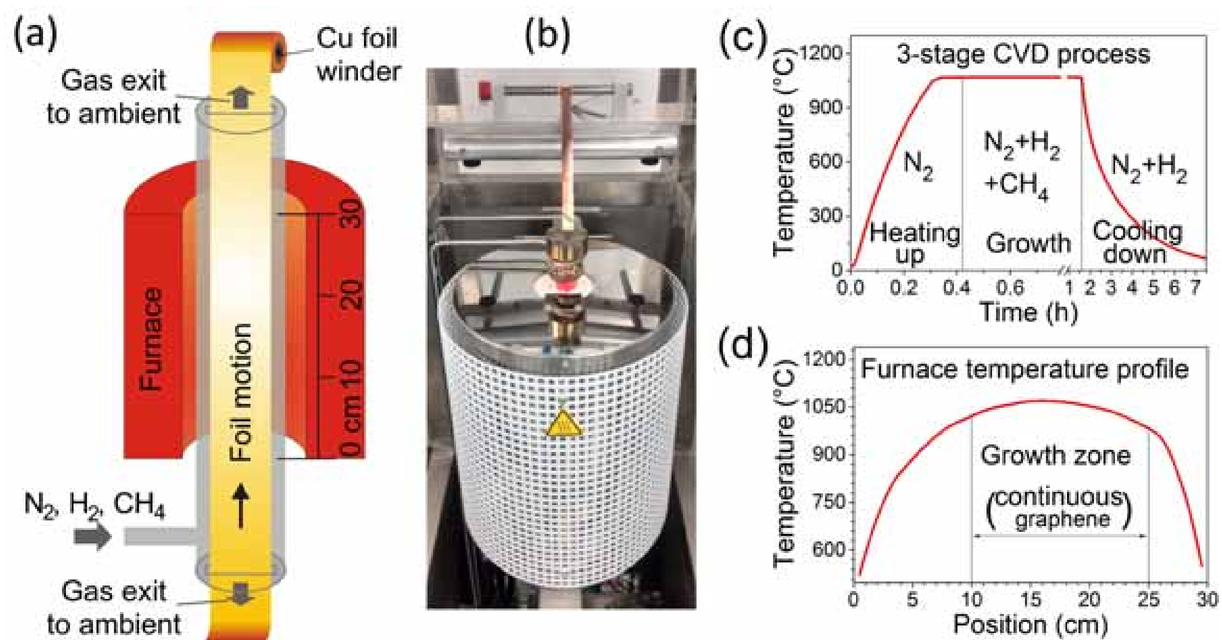

Fig. 1

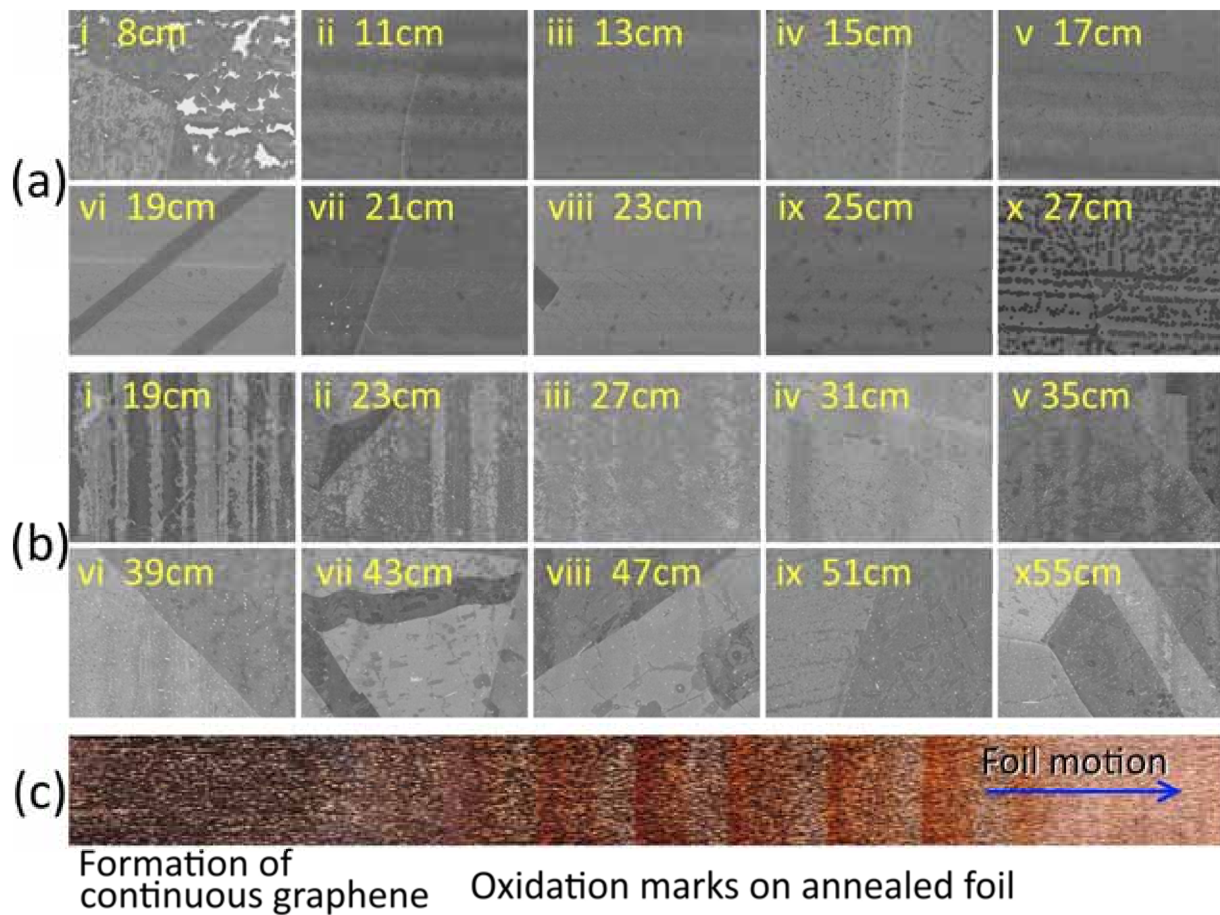

Fig. 2

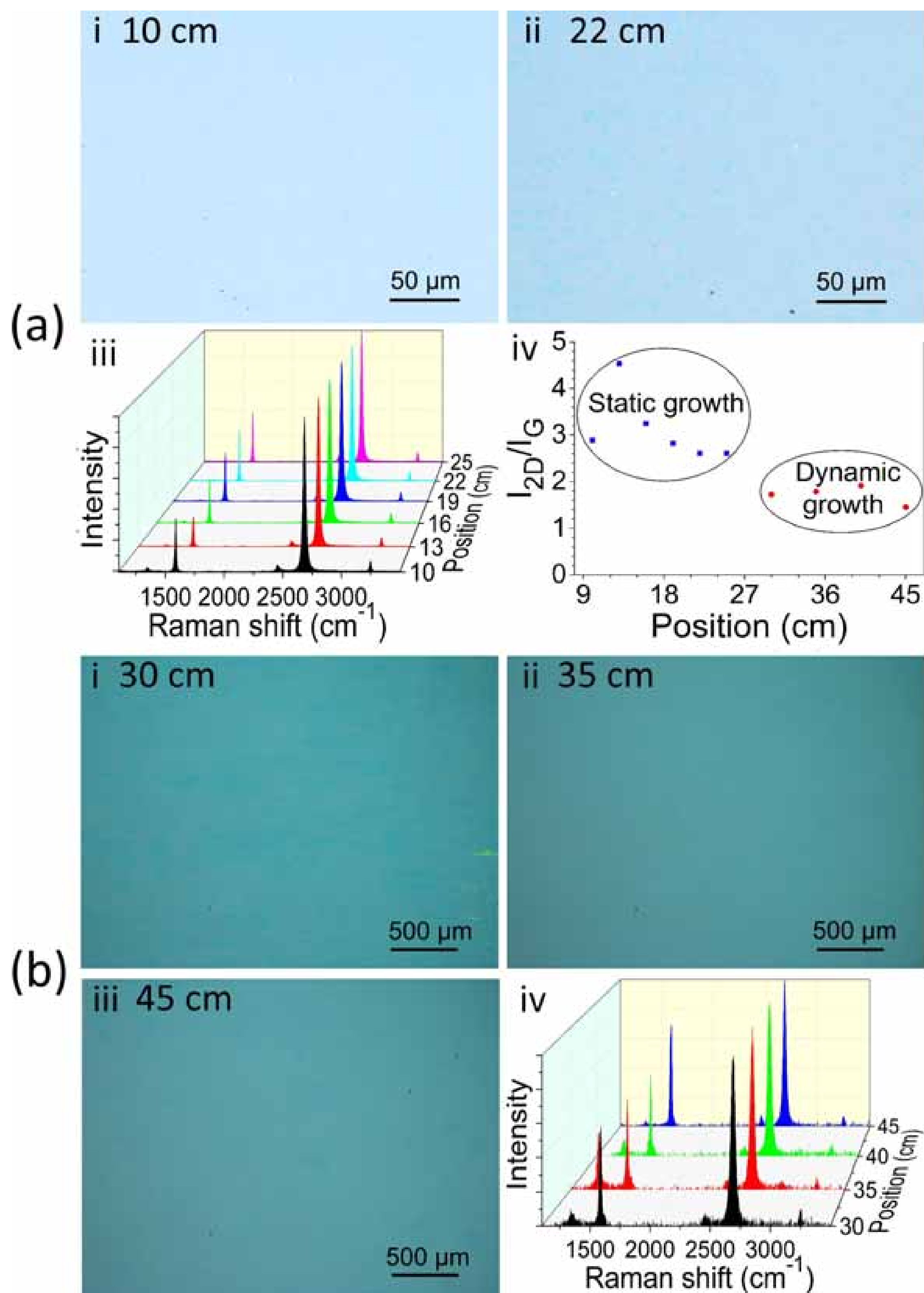

Fig. 3

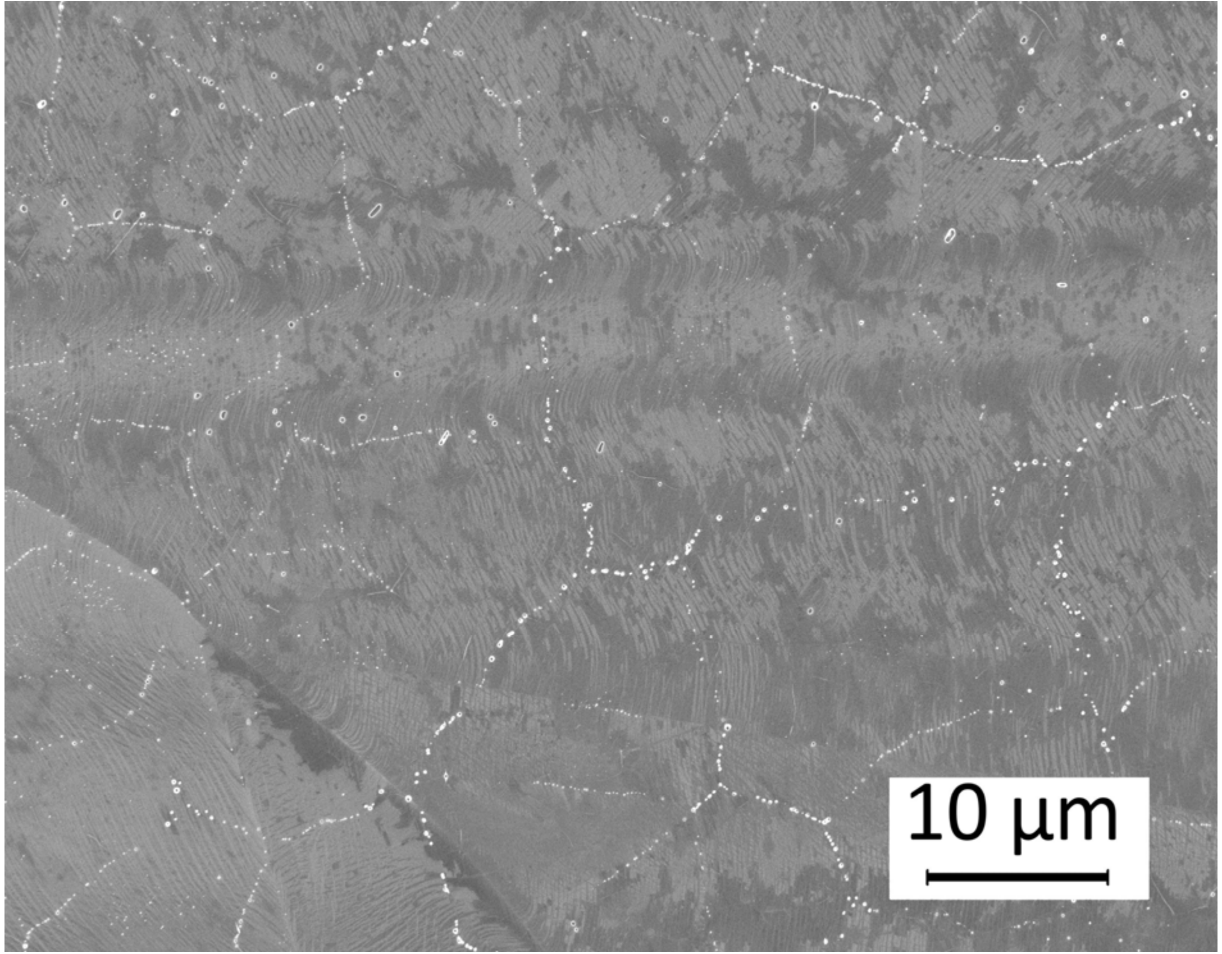
10 µm